Hindawi
Advances in Materials Science and Engineering
Volume 2017, Article ID 2715092, 10 pages
https://doi.org/10.1155/2017/2715092

Research Article

Development of Electrohydraulic Forming Process for Aluminum Sheet with Sharp Edge

Ji-Yeon Shim and Bong-Yong Kang

Carbon & Light Materials Application R&D Group, KITECH, Jeonju-si, Republic of Korea

Correspondence should be addressed to Bong-Yong Kang; kanbo@kitech.re.kr

Received 7 February 2017; Revised 18 April 2017; Accepted 13 June 2017; Published 17 July 2017

Academic Editor: Donato Sorgente

Electrohydraulic forming (EHF), high-velocity forming technology, can improve the formability of a workpiece. Accordingly, this process can help engineers create products with sharper edges, allowing a product's radius of curvature to be less than 2 mm radius of curvature. As a forming process with a high-strain rate, the EHF process produces a shockwave and pressure during the discharge of an electrical spark between electrodes, leading to high-velocity impact between the workpiece and die. Therefore, the objective of this research is to develop an EHF process for forming a lightweight materials case with sharp edges. In order to do so, we employed A5052-H32, which has been widely used in the electric appliance industry. After drawing an A5052-H32 Forming Limit Diagram (FLD) via a standard limiting dome height (LDH) test, improvements to the formability via the EHF process were evaluated by comparing the strain between the LDH test and the EHF process. From results of the combined formability, it is confirmed that the formability was improved nearly twofold, and a sharp edge with less than 2 mm radius of curvature was created using the EHF process.

1. Introduction

In the electrical appliance industry, a product layout can be designed with a relatively simple forming process. However, product design has become one of the most important factors for selecting products, so development of reproducible forming processes is needed to manufacture optimal products with sharp edges. In particular, lightweight materials such as aluminum and magnesium have been utilized for electrical appliance cases, although these materials have low formability. When attempting to form a sharp edge using conventional forming processes, these materials are often torn and wrinkled. Thus, researchers have attempted to develop new forming processes for lightweight materials with sharp edges. High-velocity forming methods have been reported to potentially increase sheet metal formability beyond the limits of conventional forming processes [1–4]. Various high-velocity forming processes have been developed, including explosive forming (EXF), electromagnetic forming (EMF), and electrohydraulic forming (EHF). Such high-strain rate forming processes result in lower tooling costs, due to the elimination of punches, which are replaced by an impulse force generated by an explosive, electromagnetic repulsion via electrical plasma channels [5]. Although EXF is one of the earliest high-velocity forming processes, handling explosives for routine research is not feasible because it is very dangerous and noisy. EMF is also limited to highly conductive materials. Therefore, EHF is the best way to form all kinds of lightweight materials.

During the EHF process, stored electrical energy is discharged to electrodes in liquid-filled chambers. A small amount of liquid between the tips of the electrodes is vaporized, forming a plasma channel. Electrical current continues to go through the channel, converting the electrical energy into the internal energy of the plasma bubble; this occurs in a very short period of time (usually less than 100 microseconds). This leads to explosive expansion of the channel by forming high-velocity shockwaves in the liquid, which forms a workpiece into a die [6]. Initial development of the EHF process began in Russia in the early 1950s by Yutkin [7]. Bruno [8] and Davies and Austin [9] reviewed early applications and research results on EHF. Specifically,

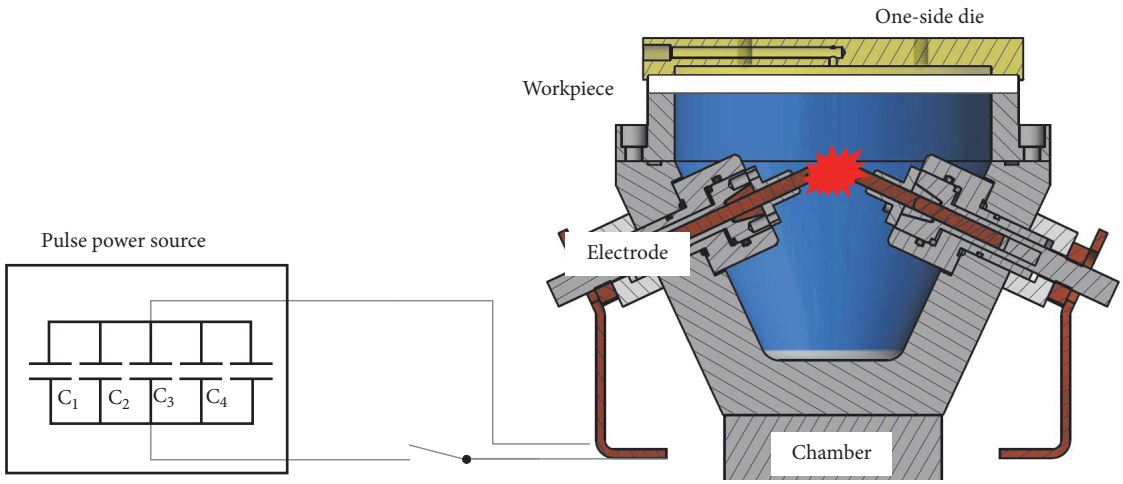

Figure 1: Cross-sectional diagram of an EHF chamber.

Bruno described a number of industrial examples where EHF machines storing 36 kJ, 60 kJ, 150 kJ, and 172 kJ were employed. However, due to the necessity of filling the chamber with liquid at the beginning of each forming cycle and evacuating the liquid at the end of it, the cycle time for the EHF process was approximately several minutes. Sanford [10] described a hybrid technology where static hydroforming was used to bulge sheet metal into the die cavity, followed by EHF, which provided a higher pressure level and filled in the details of the die cavity. According to this study, a typical cycle time for such a hybrid process is 10 minutes. More recently, Balanethiram and Daehn [3] reported an increase in the forming limit for A6061-T4 and Golovashchenko and Mamutov [11] reported forming limit improvements for DP590, DP780, and DP980. Rohatgi et al. [5] investigated the deformation behavior of A5182-O and DP590 during EHF using high-speed cameras and a digital image correlation (DIC) technique to understand the roles of the strain rate. Gillard et al. [12] analyzed the formability improvements of formability of DP780 and DP980 and developed an FE-model for EHF processes. Further, Vohnout et al. [13] reported results of pulsed loading in a closed volume, assuming energy equivalence in explosive forming. Additional simulation work fully modeling the discharge, pressure transmission, and part formation into the die has been conducted by Ford researchers [14–16]. Recently, Ahmed et al. [17] reported near 45–50% improvement to the formability of A5052-O via the EHF process [18]. According to this research, improvement to the formability of some materials, such as A6061-T4, DP590, and A5052-O, was achieved; however, EHF research on A5052-H32 sheets with low formability, which has been widely used for electrical appliances and automobiles, was not carried out. Therefore, the objective of this paper is to assess formability improvements and to attempt forming A5052-H32 sheets with sharp edges. In order to do so, an A5052-H32 FLD was drawn via an LDH test and combined with the experimental results of EHF processes. Importantly, sharp edge forming was attempted using the EHF process. Sharp edge forming is the filling of the die with a 2 mm radius of curvature. It is anticipated that this research will contribute to the manufacturing of lightweight material cases with sharp edges for small electrical appliances, such as cell phones and cameras.

2. EHF Forming System

The major advantages of high-strain rate forming processes include increases in metal formability, reduced wrinkling, reduced spring-back, and reduced manufacturing costs. EHF is a high-strain rate forming process that involves the conversion of electrical energy into mechanical energy in a liquid-filled chamber. The forming process is very fast, lasting no longer than 200 μs, and has a forming speed of approximately 300 m/s [17]. A high-strain rate during the EHF process is achieved by taking advantage of the electrohydraulic effect, which can be described as the rapid discharge of electric current between electrodes tips while being submerged in liquid-filled chambers and the propagation through the liquid of the resulting shockwave and reflective wave. The high-pressure propagation from the resulting shockwave and reflective wave causes a high-velocity impact between the workpiece and die, allowing the workpiece to be formed into the desired shape [19].

An EHF system consists of a pulse power source, chamber, electrodes, and one-sided die. Figure 1 shows a cross-sectional diagram of an EHF chamber. The necessary high voltage is obtained by charging a capacitor storage bank in a pulse power source. When the electronic trigger circuit is activated, energy is rapidly dumped into concentric or opposing spark-gap electrodes submerged in the liquid-filled chamber. The thickness of the chamber is 35 mm considering the 300 MPa fluid pressure and corrosion. A chamber with carbon steel, containing beryllium copper electrodes was used to avoid abrasion by shockwave.

3. Experimental Work

3.1. Conventional Formability Testing. An FLD is used during the design stage of any new sheet metal component for

Table 1: Material characteristics for A5052-H32.

(a) Tensile properties

Yield strength (Mpa)	Tensile strength (Mpa)	Elongation (%)	n
193	228	12	0.177

(b) Chemical composition

Component	Al	Cr	Cu	Fe	Mg	Mn	Si	Zn
Wt (%)	97	0.10	0.20	0.70	1.10	0.20	0.30	0.25

Table 2: FLD test conditions for this study.

Material	A5052-H32
Thickness (mm)	0.5
Specimen direction	Rolling direction
Temperature (°C)	25
Punch speed (mm/min)	80
Lubrication	Grease

tooling the shape and optimizing variables. In the sheet metal industry, this process is widely used and considered to be one of the most important factors for determining the formability of sheet metals. Every sheet metal has its own FLD that determines its formability, strain limit, and forming regions [20]. An FLD is a representation of the critical combination of two principal surface strains, major and minor, above which localized necking instability is observed [21]. The forming limit curve is plotted for varying strain ratios, from pure shear to equibiaxial tension. One can conclude that drawing has occurred in the case of a negative minor strain or negative strain ratio. Stretching is observed when positive minor strain is obtained, or the strain ratio is positive [22]. In order to construct the FLD, Hecker's simplified technique was employed in this study. This procedure comprises three main steps: grid marking on the workpiece, punch stretching of the grid marked workpiece to failure (onset of localized necking), and strain measurement on the deformed specimens [23]. In order to evaluate the formability, a 0.5 mm thick A5052-H32 (NOVELIS) sheet was considered. The tensile properties and chemical composition of the workpiece are shown in Table 1. Eight workpieces, ranging from 25 mm × 200 mm to 200 mm × 200 mm, were cut from one sheet. Square (2 mm × 2 mm) grid patterns were imprinted on the workpieces for strain measurement after forming. The formability testing equipment consists of a hemispherical punch of 101.6 mm in diameter, as well as a lower and upper die on a 20-ton hydraulic press. Table 2 shows the basic forming conditions of the FLD test. For better accuracy, experiments were conducted three times and major and minor strain values were taken into account. After forming, grids on the workpiece in and around the necked regions were imaged, and major and minor engineering strain components were calculated from the grid pattern analyzer. The grid pattern analyzer is comprised of a video camera system for data acquisition and software for data process and analysis. The basic procedure for measuring strain data with the grid pattern analyzer is the following:

(i) A grid pattern is applied to an undeformed blank.

(ii) The blank is formed.

(iii) The grid pattern analyzer is used to image a single grid element.

(iv) From the image, the computer determines major and minor strain values.

3.2. EHF. The EHF formability experiments in this study were conducted from a flat blank, and the die cavity was filled using a single EHF pulse. In this study, a conical EHF chamber was used in conjunction with the conical die to form the workpiece in a state of biaxial strain. Figure 2 shows the conical die for the EHF process. Using an electrochemical etching process, square grid patterns (2.0 mm × 2.0 mm) were marked on the workpiece to measure strain after forming.

The electrodes can be seen above, passing through the chamber walls. They were insulated from the walls by a nonconductive polymeric material with good mechanical resiliency in order to withstand the intense dynamic loading occurring within the chamber. A hemispherical chamber with a 200 mm diameter was filled with 2 L of tap water for the EHF. The electrode gap in the chamber was 20 mm, and a copper bridge wire, 0.3 mm in diameter, was placed between the electrode tips before each pulse in order to promote efficient and repeatable discharge performance.

During the EHF process, a workpiece was installed at the top of the chamber and then clamped by an o-ring and press. The air remaining in the die was removed by a vacuum pump. The chamber was filled with water up to its upper rim. The pulse power source had a maximum energy capacity of 60 kJ, and the electrical energy used in the EHF ranged from 0.3 kJ to 8 kJ. Electrical energy was stored in high voltage capacitors and charged through a transformer and a set of diodes. Each of them was connected to the discharge circuit through their respective vacuum switches. A set of vacuum switches closed the circuit and delivered the voltage stored in each module of the capacitors to the electrodes. Moreover, a Rogowski coil for measuring the currents on electrodes was set at the ends of the electrodes. The Rogowski coil measured the current linearly, from low to high current, using mutual inductance. It can also measure the current in a wide frequency range. Figure 3 shows the set-up for the EHF process.

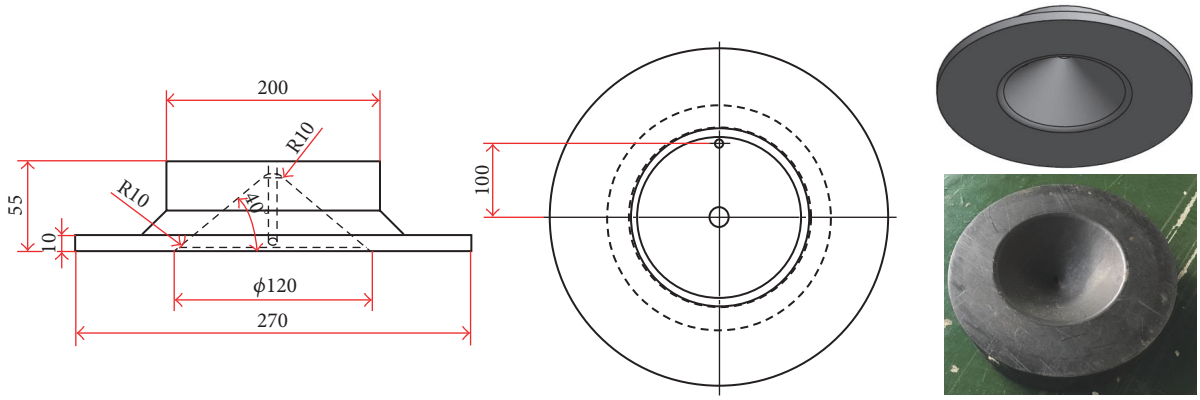

Figure 2: Die for EHF.

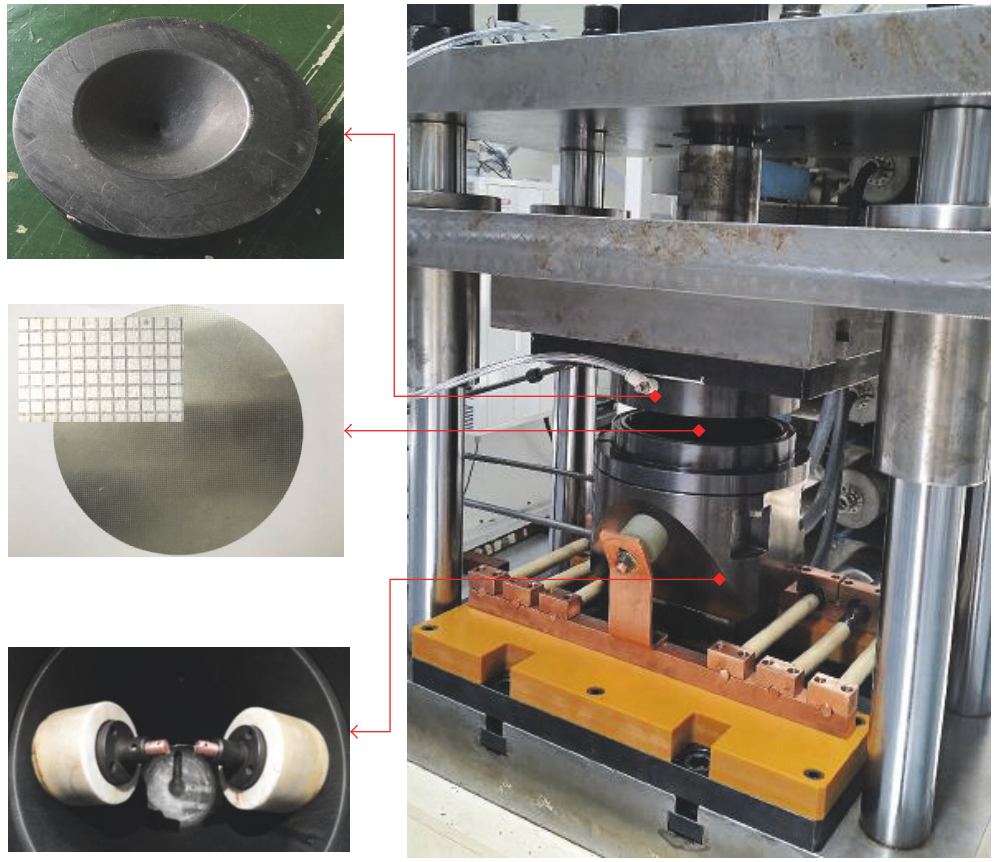

Figure 3: Set-up for EHF.

Generally, the parameters that define the efficiency of the EHF process are the mutual positions of the electrodes, electrical properties of the liquid, charging voltage, capacitance of the circuit, inductance and resistance of the equipment and connecting cables, volume of the chamber, and the distance between the discharge channel and workpiece [17]. In this study, all parameters except charging voltage were set under the same conditions. Table 3 shows the EHF conditions.

3.3. Results and Discussion. To draw the FLD after a dome stretching test, workpieces were measured in terms of major and minor engineering strain. Figure 4 shows the deformed workpiece after the LDH test. From these deformed grids, the FLD, consisting of major and minor strains, was plotted using a grid pattern analyzer. All of the LDH specimens were formed until failure, and the grid with the largest uniform major strain was always located near the cracks. If

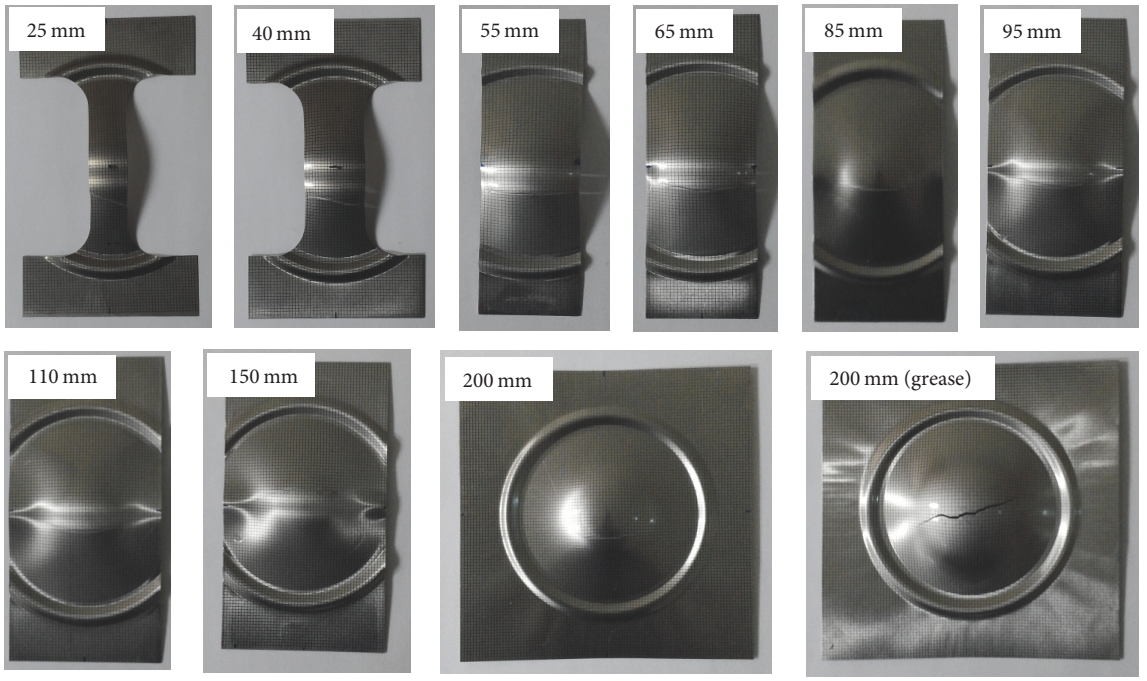

Figure 4: Workpieces after dome stretching test.

Table 3: EHF conditions.

Capacitance (μF)	Charging voltage (kV)	Charging energy (kJ)	Electrode gap (mm)
64	1	0.3	20
	2	1.2	
	3	2.8	
	4	5.1	
	5	8	

the measured square grid was located near the crack on a specimen, then that grid was marked as *Failed*. Conversely, if a square grid was located a safe distance away from the crack, then that grid was marked as *Safe*.

The typical areas with the highest strain concentrations were located on or near a crack. Figure 5 shows the static FLD for A5052-H32 from the results of the LDH test. Table 4 shows the resulting measurements of the dome height after the LDH test (repeated 3 times). The maximum dome height was 19.18 mm in workpieces with 25 mm × 200 mm dimensions and a minimum of 13.22 mm at 110 mm × 200 mm in dry conditions. When the dome stretching test was performed with lubrication, the dome height was 23.27 mm for workpieces with 200 mm × 200 mm dimensions.

Figure 6 shows the setting for measuring the waveform, wherein measured voltages can calibrate the input current of the electrodes. The discharge times were similar (25 μs) for all EHF conditions. The measured waveforms increased in direct relation to the charging voltage. Each measured voltage was 1.2 mV, 1.7 mV, 2.2 mV, 2.8 mV, and 3.2 mV at 1 kV, 2 kV, 3 kV, 4 kV, and 5 kV, respectively. Therefore, input currents for the

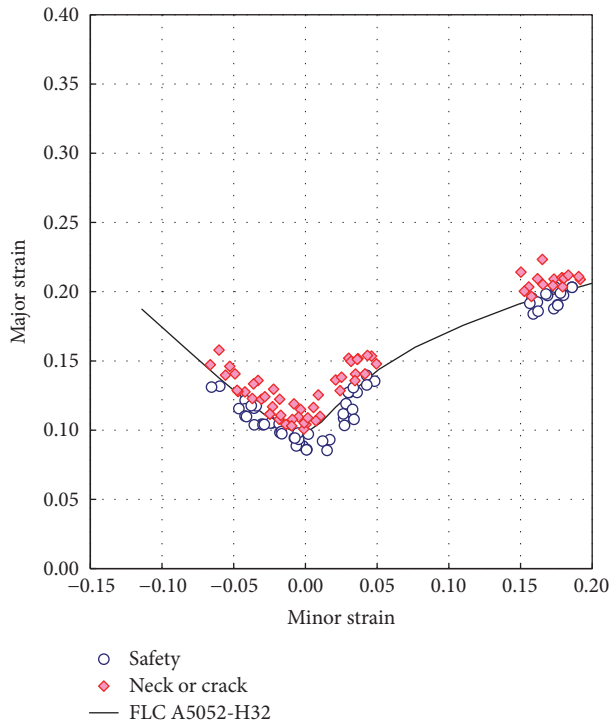

Figure 5: FLD of A5052-H32.

EHF process were calculated as 30 kA, 42.5 kA, 55 kA, 70 kA, and 80 kA, by a calibration coefficient of 25 kA/mV. Based on this result, it could be determined that increasing the currents would lead to an increase in the shockwave within the chamber during the EHF process.

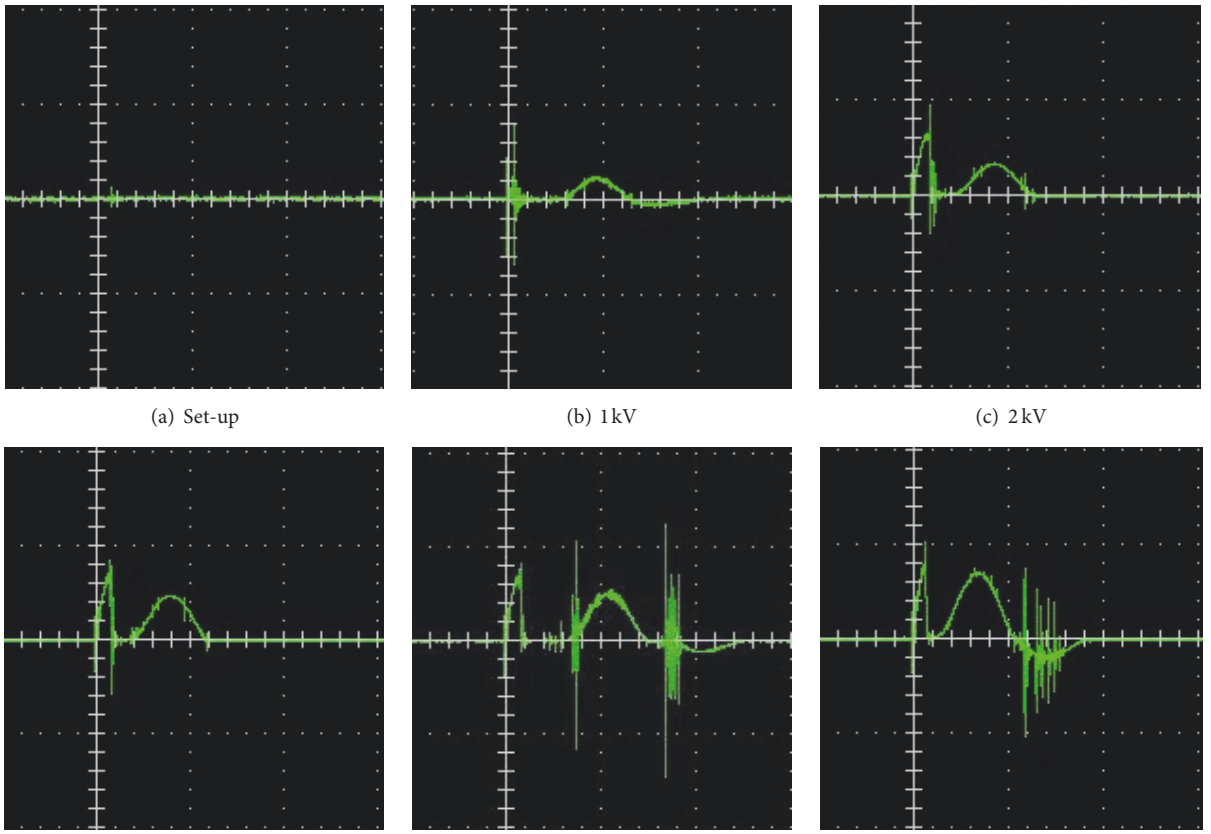

(a) Set-up (b) 1 kV (c) 2 kV

(d) 3 kV (e) 4 kV (f) 5 kV

Figure 6: Discharge waveform (X: 200 μs/div, Y: 500 mV/div) with a calibration coefficient of 25 kA/mV.

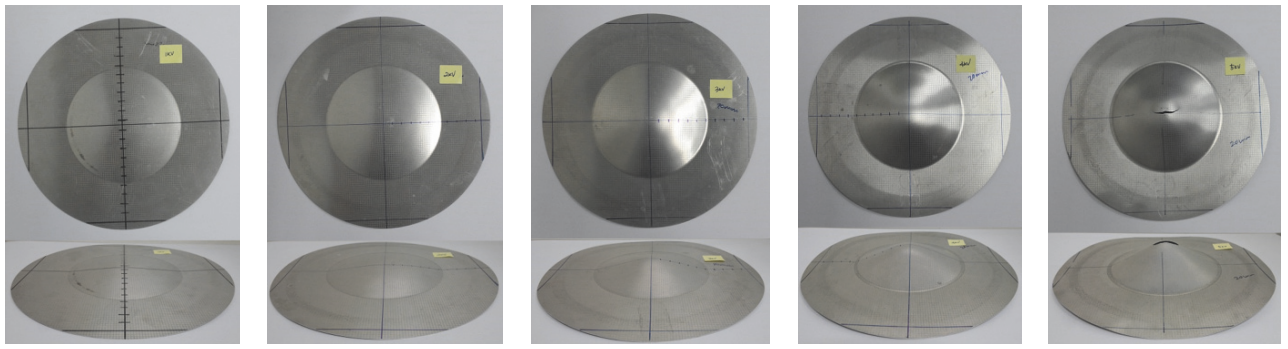

(a) 1 kV (b) 2 kV (c) 3 kV (d) 4 kV (e) 5 kV

Figure 7: Workpieces after EHF.

Figure 7 shows the deformed workpieces after EHF. A crack was observed under a 5 kV charging voltage at the apex of the workpiece. Table 5 shows the height of the deformed workpiece, from flat to apex, under different charging voltage conditions, after being measured precisely using a height gauge.

Dome height was measured as 5.03 mm, 8.39 mm, 12.03 mm, 19.31 mm, and 28.36 mm at 1 kV, 2 kV 3 kV, 4 kV, and 5 kV charging voltage, respectively, as shown in Table 5. The dome height was increased in direct relation to the charging voltage. As shown in Figure 8, deformed workpiece profiles at 2 kV and above increased sharply. This confirmed that the dome height of the EHF workpiece was increased in direct relation to the charging voltage, because the charging voltage provides the formation energy. Therefore, increasing the charging voltage generated an increased shockwave and reflected wave in the chamber, leading to an increase in the dome height of the workpiece.

To validate the formability improvement using EHF, strain in the workpiece after a 5 kV charging voltage was

Table 4: Dome height from the LDH test (unit: mm).

Size	Height
25 × 200	19.14
	19.01
	19.18
40 × 200	18.80
	19.00
	18.75
55 × 200	19.12
	19.03
	19.10
65 × 200	17.11
	16.19
	17.05
85 × 200	13.45
	14.00
	13.47
95 × 200	13.54
	13.81
	13.66
110 × 150	13.22
	13.46
	13.48
150 × 200	16.47
	16.62
	16.39
200 × 200	17.89
	17.51
	17.76
200 × 200 (Grease)	23.02
	23.17
	23.27

Table 5: Dome height from EHF.

Charging voltage (kV)	Charging energy (kJ)	Height (mm)
1	0.3	5.03
2	1.2	8.39
3	2.8	12.03
4	5.1	19.31
5	8	28.36

measured and plotted together, along with the static FLC via an LDH test, as shown in Figure 9. The 5 kV EHF workpiece had higher major strain than workpieces using the LDH test. Combinations of FLD for both parts showed that the workpieces using EHF had higher formability than those from the LDH test. The maximum dome height in the LDH test was measured at 23.27 mm in lubricated workpieces with dimensions of 200 mm × 200 mm, whereas the maximum dome height using an EHF test was measured at 28.36 mm with a 5 kV charging voltage. These results were mainly due to a high-velocity plasma channel leading to improved formability in the workpiece. The approximate improvement in formability was measured as 28% more than that of conventional forming processes.

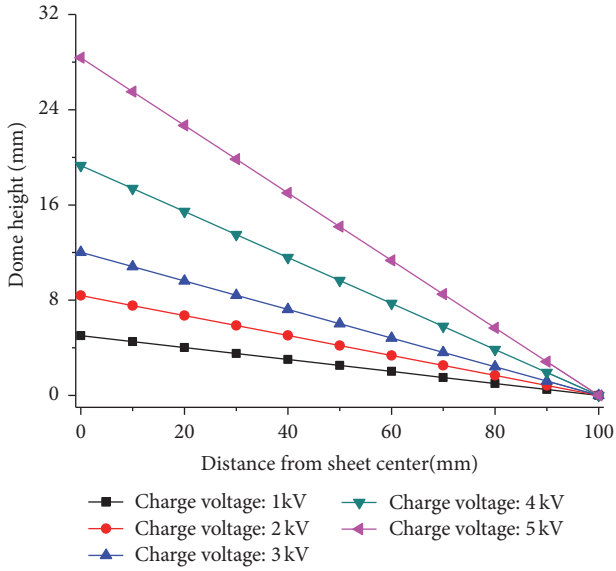

Figure 8: Height profile of the deformed workpieces after EHF.

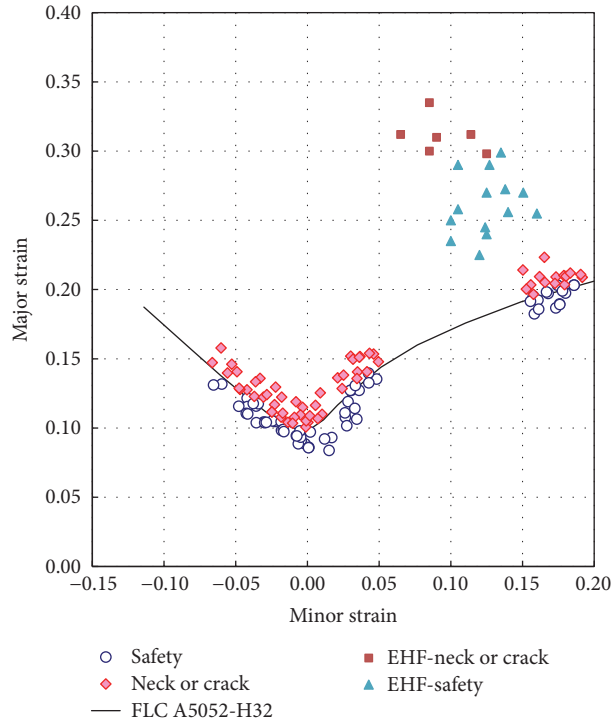

Figure 9: Combined formability results for A5052-H32, 0.5 mm.

4. EHF with Sharp Edges

A case with a 175 mm diameter, 5 mm height, and a less than 2 mm radius of curvature was selected as a lightweight material case with sharp edges for small electric appliances. To assess the possibility of sharp edge forming via traditional press forming, a simple press forming simulation consisting of a punch, die, and workpiece was performed using a measured FLD of A5052-H32. The press forming die's radius

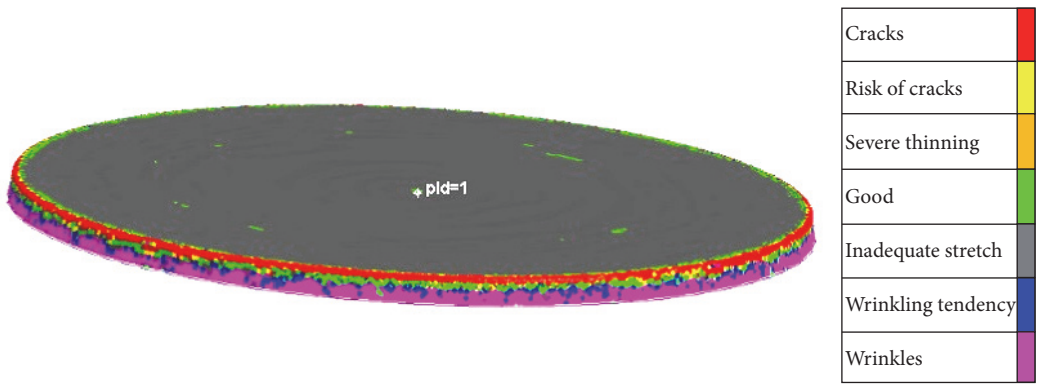

Figure 10: Cracks and wrinkles by press forming.

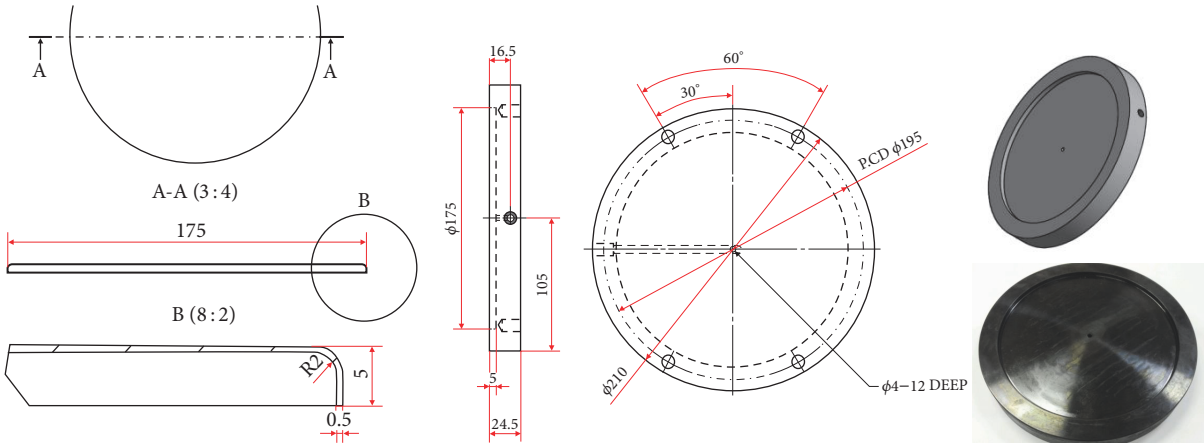

(a) Desired sharp edge (b) Die

Figure 11: Target and die for sharp edge forming.

of curvature was 2.0 mm. As a result, it was predicted to crack and wrinkle along the circumference of the edge, as shown in Figure 10.

Figure 11 shows the target case and designed die for EHF. As a die material, SKD11 was employed with a 50HRC via heat treatment. In particular, the radius of curvature of the die was machined at 0.5 mm to achieve a minimum radius of curvature on the forming part. The workpiece was located at the top of the chamber, and water leakage was prevented by a rubber-ring and hydraulic press. After setting up the experiment, a 10 kV charge was run through a pulse power source; then, charged electrical energy was discharged into the electrodes. The damped sinusoidal waveform was measured as shown in Figure 6. The discharge time and peak current were measured at 25 μs and 153 kA, respectively. To evaluate the radius of curvature on the edge of the circumference, inner radius measurements were precisely performed using a 3D scanner, as shown in Figure 12. The radius of curvature was measured in 50 mm intervals. Figure 13 shows the radius of curvature on the edge of the circumference. The radius of curvature was measured to be less than 1.5 mm for all points; however, the radius of some points located adjacent to the electrodes was less than 1.0 mm. Although the radius of the edge was nonuniform, due to the nonuniform distribution of pressure applied on the workpiece by a shockwave and reflective wave, the EHF process could achieve a sharp edge of less than 2.0 mm for a lightweight materials case.

5. Conclusions

Improvements to formability using the EHF process were verified by comparing conventional forming and EHF, leading to the following conclusions:

(1) An FLD of 0.5 mm thickness A5052-H32 was drawn by an LDH test. A 28% improvement of formability was verified by comparing the measured strain between the LDH test and EHF in combinations of FLD. According to the formability improvement, a maximum dome height using EHF was approximately 5 mm higher than when using the LDH test.

(2) EHF was performed under different charging voltages via waveform measurement. Although the charging voltage was discharged for 25 μs under all EHF conditions, a peak current was increased to approximately 11 kA in direct relation to the charging voltage. In particular, dome heights were increased as charge voltage increased, meaning that

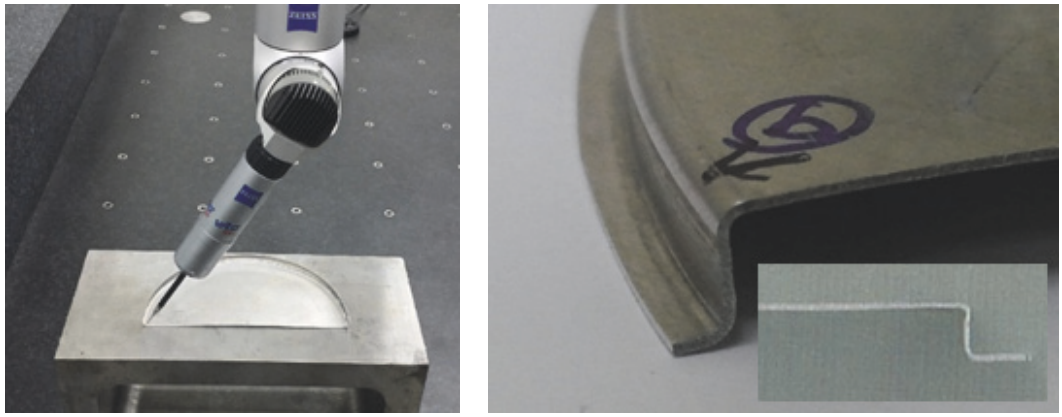

(a) 3D scanning (b) Sharp edge

Figure 12: 3D scanning and forming part with sharp edge.

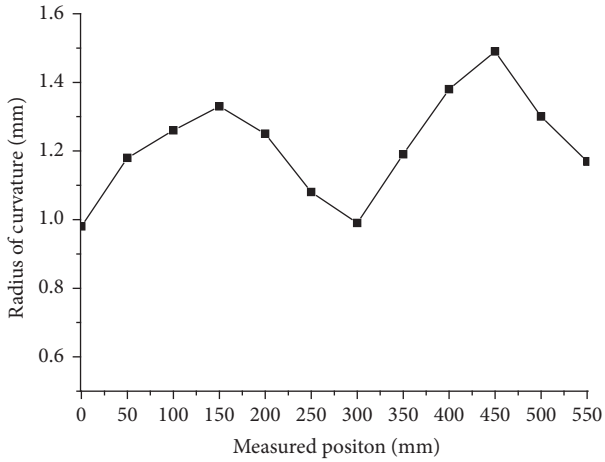

Figure 13: Radius of curvature on sharp edge.

increasing the charge voltage caused a greater shockwave and reflected wave in the chamber, which led to an increase in the formability of the workpiece

(3) For applying the EHF process to small electric appliances, a circular formed part with sharp edges of less than 2 mm in radius of curvature was manufactured. The radius of curvature was verified using a 3D scanner. Although all radii of curvature did not have the same radius, the radius of curvature was less than 1.5 mm for all curvatures on the manufactured components.

Conflicts of Interest

The authors declare that they have no conflicts of interest.

References

[1] V. Psyk, D. Risch, B. L. Kinsey, A. E. Tekkaya, and M. Kleiner, "Electromagnetic forming—a review," *Journal of Materials Processing Technology*, vol. 211, no. 5, pp. 787–829, 2011.

[2] D. J. Mynors and B. Zhang, "Applications and capabilities of explosive forming," *Journal of Materials Processing Technology*, vol. 125-126, pp. 1–25, 2002.

[3] V. S. Balanethiram and G. S. Daehn, "Hyperplasticity: increased forming limits at high workpiece velocity," *Scripta Metallurgica et Materiala*, vol. 30, no. 4, pp. 515–520, 1994.

[4] S. F. Golovashchenko, "Material formability and coil design in electromagnetic forming," *Journal of Materials Engineering and Performance*, vol. 16, no. 3, pp. 314–320, 2007.

[5] A. Rohatgi, E. V. Stephens, A. Soulami, R. W. Davies, and M. T. Smith, "Experimental characterization of sheet metal deformation during electro-hydraulic forming," *Journal of Materials Processing Technology*, vol. 211, no. 11, pp. 1824–1833, 2011.

[6] A. V. Mamutov, S. F. Golovashchenko, J. J. Bonnen, A. J. Gillard, S. A. Dawson, and L. Maison, "Electrohydraulic forming of light weight automotive panels," in *Proceedings of the 7th International Conference on High Speed Forming*, pp. 115–124, 2016.

[7] L. A. Yutkin, Electrohydraulic effect, Mashgiz, Translation No. AD-267-722. Armed Services Technical information Agency, Arlington Hall Station, Arlington, 1955.

[8] E. J. Bruno, "High-velocity forming of metals," *American Society of Tool and Manufacturing Engineers*, 1968.

[9] R. Davies and E. R. Austin, *Development in high speed metal forming*, Industrial Press Inc, 1970.

[10] J. E. Sanford, "High velocity takes off again," *Iron Age*, vol. N3, pp. 91–95, 1969.

[11] S. F. Golovashchenko and V. S. Mamutov, "Electrohydraulic forming of automotive panels," in *Proceedings of the 6th Global Innovations Symposium: Trends in Materials and Manufacturing Technologies for Transportation Industries*, T. R. Bieler, J. E. Carsley, H. L. Fraser, J. W. Sears, and J. E. Smugeresky, Eds., pp. 65–70, San Francisco, Calif, USA, 2005.

[12] A. J. Gillard, S. F. Golovashchenko, and A. V. Mamutov, "Effect of quasi-static prestrain on the formability of dual phase steels in electrohydraulic forming," *Journal of Manufacturing Processes*, vol. 15, no. 2, pp. 201–218, 2013.

[13] V. J. Vohnout, G. Fenton, and G. S. Daehn, "Pressure heterogeneity in small displacement electrohydraulic forming process," in *Proceedings of 4th International Conference on High Speed Forming*, G. Daehn, Ed., pp. 65–74, Columbus, Ohio, USA, 2010.

[14] S. F. Golovashchenko, A. V. Mamutov, J. J. F. Bonnen, and A. J. Gillard, "Electrohydraulic forming of sheet metal parts," in *Proceedings of the International Conference on Technology of Plasticity*, G. Hirt and A. E. Tekkaya, Eds., pp. 1170–1175, Aachen, Germany, 2011.

[15] J. J. F. Bonnen, S. F. Golovashchenko, S. A. Dawson, A. V. Mamutov, and A. J. Gillard, "Electrohydraulic sheet metal forming of aluminum panels," in *Proceedings of the TMS Light Metals 2012 Conference*, pp. 449–454, Orlando, Fla, USA, March 2012.

[16] A. Hassannejadasl, D. E. Green, S. F. Golovashchenko, J. Samei, and C. Maris, "Numerical modelling of electrohydraulic free-forming and die-forming of DP590 steel," *Journal of Manufacturing Processes*, vol. 16, no. 3, pp. 391–404, 2014.

[17] M. Ahmed, D. R. Kumar, and M. Nabi, "Enhancement of formability of AA5052 alloy sheets by electrohydraulic forming process," *Journal of Materials Engineering and Performance*, vol. 26, no. 1, pp. 439–452, 2016.

[18] T. Mane, V. Goel, and S. D. Kore, "Finite element modelling of electro-hydraulic forming of sheets," *Procedia Materials Science*, vol. 6, pp. 105–114, 2014.

[19] S. F. Golovashchenko, A. J. Gillard, D. A. Cedar, and A. M. Ilinich, "Electrohydraulic forming tool," an applicant for a patent: Ford Global Technologies, Llc, US7516634B1.

[20] S. D. Kumar, T. Amjith, and C. Anjaneyulu, "Forming limit diagram generation of aluminum Alloy AA2014 using Nakazima test simulation tool," *Procedia Technology*, vol. 24, pp. 386–393, 2016.

[21] B. Şanay, Prediction of plastic instability and forming limits in sheet metal forming, The Master degree thesis in the graduate school of Middle East Technical University (2010) 24–27.

[22] S. D. Kumar, T. R. Amjith, and C. Anjaneyulu, "Forming limit diagram generation of aluminum alloy AA2014 using Nakazima test simulation tool," *Procedia Technology*, vol. 24, pp. 386–393, 2016.

[23] S. S. Hecker, "Simple technique for determining forming limit curves," *Sheet Metal Industries*, vol. 52, no. 11, pp. 671–676, 1975.